Environmental Science

AIMS Environmental Science, 13(5): 917–935.
DOI: 10.3934/environsci.2026036
Received: 28 February 2026
Revised: 19 September 2026
Accepted: 20 September 2026
Published: 24 September 2026

http://www.aimspress.com/journal/environmental

Research article

Autotrophic denitrification characteristics of urban wastewater treatment plant effluent driven by sodium thiosulfate siderite

Yong Chen[1,2], Xiaoli Wen[3], Geran Zhao[1], Chengcai Zhang[1,*]

[1] Zhengzhou University, Zhengzhou City, Henan Province 450001, China
[2] Henan University of Engineering, Zhengzhou City, Henan Province 451191, China
[3] Zhengzhou Institute of Food Technology. Zhengzhou city, Hennan Province 451162, China

* **Correspondence:** Email: zhangcc@zzu.edu.cn.

Abstract: Autotrophic denitrification has garnered increasing attention as it eliminates the dependency on external organic carbon sources. Addressing the challenge of elevated nitrate levels in the tailwater of urban wastewater treatment plants (WWTPs), we proposed a sodium thiosulfate-siderite autotrophic denitrification (STSAD) biofilter for advanced nitrogen removal. The optimal operational parameters were an influent pH of 7.0, a temperature of 30°C, a hydraulic retention time (HRT) of 2 hours, and a sodium thiosulfate dosage equivalent to 1.5 times the theoretical requirement. Under these conditions, the system achieved a nitrate (NO_3^--N) removal rate of 100% and a total nitrogen (TN) removal efficiency exceeding 95%. Microbial analysis revealed significant biofilm enrichment on the ceramsite and siderite media, with *Thiobacillus* and *Ferritrophicum* identified as the predominant denitrifying genera. This ensured that effluent TN and COD levels comply with discharge standards.

Keywords: tailwater from urban wastewater treatment plant; STSAD system; Sulfur/iron-driven autotrophic denitrification; Sulfur autotrophic denitrifying microbial population

1. Introduction

Excessive nitrogen not only leads to the eutrophication of water bodies but also causes harm to animals and humans [1]. Increasing attention has been given to the effective deep treatment of tailwater. Although the concentration of tailwater in sewage treatment plants is relatively low, it

contains refractory organic compounds, NH_4^+-N and NO_3^--N [2,3]. Therefore, deep denitrification of sewage plant tailwater is of great importance.

Biological denitrification is an economical and efficient technology, making it the most widely used method for nitrogen removal in urban sewage treatment [4]. Compared with heterotrophic systems, autotrophic denitrification systems offer several advantages. Among these, sulfur-oxidizing autotrophic denitrifiers utilize nitrate as an electron acceptor to oxidize reduced sulfur compounds (e.g., H_2S, $S_2O_3^{2-}$, and S^0) into sulfate (SO_4^{2-}) [5]. By eliminating the requirement for exogenous organic carbon sources, this process minimizes sludge production and mitigates N_2O emissions [6].

A sulfur-limestone packed bed reactor is the most common configuration for sulfur autotrophic denitrification. Yingying Li et al. [7] operated a pilot-scale sulfur-limestone autotrophic denitrifying biofilter for municipal tailwater treatment. They found that at a hydraulic retention time (HRT) of 18 hours and temperatures ranging from 6.4°C to 9.8°C, the TN and NO_3^--N removal rates reached 81.1% and 85.3%, respectively. Similarly, Ahmed et al. [8] used a pilot-scale sulfur-limestone packed bed reactor to treat municipal domestic sewage. When the influent nitrate nitrogen load was 360 mg/(L·d) and 180 mg/(L·d), the reactor achieved removal rates of 89% and 79%, respectively, indicating a robust denitrification performance. However, while limestone provides alkalinity and an inorganic carbon source, it cannot act as an electron donor. Furthermore, the presence of limestone increases water hardness [9], highlighting the need to develop novel buffering and inorganic carbon sources.

Siderite ($FeCO_3$), one of the most widely distributed minerals in nature, has shown great potential. Under anoxic conditions, autotrophic denitrifying microorganisms can use Fe^{2+} as an electron donor to reduce NO_3^--N to N_2 [10,11]. Studies on the simultaneous removal of nitrate and phosphate via siderite-based autotrophic denitrification confirmed that siderite is a highly effective electron donor for nitrate removal. Zhu et al. [12,13] coupled sulfur and siderite autotrophic denitrification to enhance nitrate removal. Their results demonstrated that this coupled system outperformed the traditional sulfur-limestone system, achieving a denitrification rate of 720.35 mg/(L·d) [14]. $FeCO_3$ not only provides alkalinity and inorganic carbon but also participates in the denitrification process as an electron donor, significantly improving reactor performance [15].

Sodium thiosulfate is a common, highly water-soluble chemical. Capua et al. [16] found that thiosulfate can achieve a relatively high denitrification rate (52.5 mg/(L·d) NO_3^--N) with an S/N ratio of 1.8, which is 10 times higher than that of elemental sulfur (S^0). Cardoso [17] also reported that, compared with S^0 and S^{2-}, the nitrate removal rate using thiosulfate increases by 4.58 and 9.45 times, respectively. These findings indicate that using sodium thiosulfate as an autotrophic sulfur source offers significant advantages, maintaining high efficiency even at concentrations up to 2200 mg/L.

In summary, research on advanced nitrogen removal primarily entails optimizing biological processes and developing new electron donors. However, challenges such as high energy consumption and excessive sludge production remain. Moreover, autotrophic nitrogen removal technologies (e.g., sulfur and iron autotrophy) have garnered much attention due to their independence from organic carbon sources. Nevertheless, their application is often limited by electron donor efficiency and the accumulation of by-products.

In this study, a novel approach utilizing a dual electron donor synergy is adopted. Ferrous ions (Fe^{2+}) are provided as the primary electron donor, while carbonate ions (CO_3^{2-}) are simultaneously released to buffer the pH, solving the issue of external limestone addition in traditional sulfur autotrophic systems. Sodium thiosulfate ($Na_2S_2O_3$) is used as a highly soluble sulfur source ($S_2O_3^{2-}$). Its denitrification rate is 10 times that of elemental sulfur (S^0), and it maintains high efficiency even under low-temperature and low S/N ratio conditions. The combination of siderite (not "pyrite") and sodium thiosulfate optimizes the electron transfer pathway, achieving a nitrogen removal rate of

720.35 mg/(L·d) [14], which is significantly higher than that of the traditional sulfur-limestone system. Ceramic particles are utilized to provide a high specific surface area, promoting biofilm formation [17]. Siderite continuously releases $Fe^{2+}$and CO_3^{2-}, enhancing system stability [18,19]. High-throughput sequencing reveals that sulfur-oxidizing bacteria (e.g., Thiobacillus) and iron-oxidizing bacteria (e.g., Ferrovum) form a symbiotic relationship, synergistically improving nitrogen removal efficiency. Here, we introduce an innovative strategy by combining sodium thiosulfate with siderite; the fundamental innovation lies in the complementary chemical properties of this specific combination: soluble sodium thiosulfate can bypass the dissolution rate limiting step of solid sulfur, thereby providing an instant electron donor for rapid denitrification processes. The oxidation of siderite consumes protons, effectively buffering the acidic environment generated by the oxidation of thiosulfate. This creates a self-balancing pH environment, which is conducive to the enrichment of neutral denitrifying bacteria (such as Thiobacillus and Ferritrophicum), reducing the need for external alkalinity adjustment compared to pure sulfur-based systems.

2 Materials and methods

2.1. Reactor setup

For the experiment setup, we adopted a reactor unit, as shown in Fig. 1. The reactor unit was self-processed, and the material was plexiglass. The reactor radius was 50 mm, the height was 1000 mm, the effective volume was 1.9 L, the cushion layer height was 100 mm, the packing height was 700 mm, and the path included a sampling mouth every 100 mm for a total of seven sampling mouths.

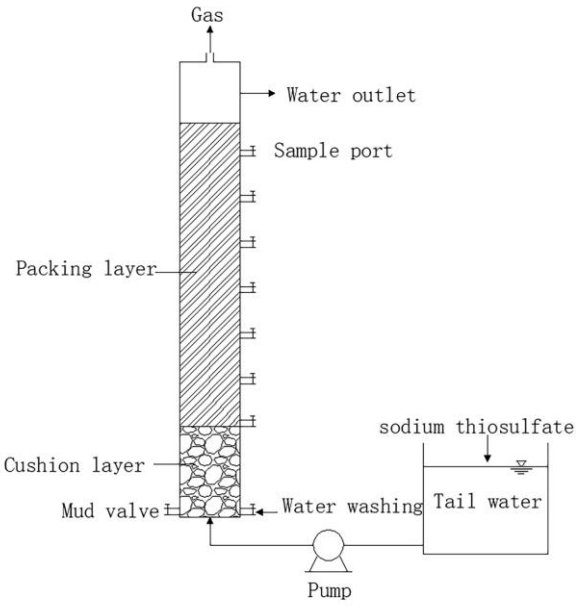


Figure 1. Reactor schematic diagram

The packing layer in reactor were ceramsite and siderite (diameter 3-5 mm), and the By volume of the two was 1:1. At bottom of column was an inlet, a sludge valve, and a water flushing device, and at the top was a gas outlet and a water outlet. Among them, a liquid flowmeter was used to control flow backwash water, and the backwash cycle was initiated based on the increase in resistance caused

by the interception of pollutants during operation. The influent was pumped into the reactor via a peristaltic pump, utilizing a bottom-inlet and top-outlet configuration.

There were two fillers in this experimental reactor: ceramsite (a) and siderite (b). The ceramsite (3-5 mm in particle size) was synthesized from shale and was purchased from Wanyuan Water Purification Material Co., Ltd., Henan, China. The siderite particles (3-5 mm) were purchased from Gongyi Zijing Longteng Filter Media Distribution Department, Henan, China. The actual mineral phase of the siderite was $FeCO_3$ (ferrous carbonate), which served as the electron donor in this study. Moreover, while X-ray fluorescence (XRF) analysis conventionally reported total iron content as Fe_2O_3, the mineral was chemically composed of $FeCO_3$ rather than ferric oxide. XRF analysis indicated that the elemental composition of the natural siderite sample mainly included Fe, Si, Mn, Al, Zn, Mg, and Ca. The detailed elemental composition is summarized in Table 1.

Table 1. XRF analysis of the siderite.

Chemical composition	Fe_2O_3	SiO_2	CaO	Al_2O_3	ZnO	MnO	MgO	other
Mass fraction (%)	43.26	21.22	11.76	6.70	5.09	3.52	1.41	7.04

The Fe_2O_3content reported in this table represents the total iron content expressed asFe_2O_3 equivalent.

The water required for the test was taken from the Wulongkou sewage treatment plant, Zhengzhou City, Henan Province, China. We acquired water at a regular time every day, and the water quality of the tailwater was relatively stable. The characteristics of inlet water quality are shown in Table 2.

Table 2. Water quality characteristics of the influent.

Index	Numerical value	Index	Numerical value
COD	35-45 mg/L	NO_2^--N	0.005-0.01 mg/L
TN	7.2-7.8 mg/L	NH_4^+-N	0.1-0.3 mg/L
NO_3^--N	6.6-7.2 mg/L	pH	6.8-7.5

With the increasing environmental protection requirements, the demand for total nitrogen is becoming higher and higher. In some areas, sewage treatment plants are required to discharge wastewater into the watershed according to surface water environmental quality standards. Additionally, total nitrogen is required to be further reduced.

In the experiment, the sludge used during the start-up phase of reactor was taken from anaerobic tank of Wulongkou Sewage-treatment plant in Zhengzhou. The total suspended concentration of sludge was about 13000mg/L. Each reactor was inoculated with 500mL of anaerobic sludge for domestication.

2.2. Experimental scheme

First, an autotrophic denitrification reactor was constructed, anaerobic tank sludge was added for domestication culture, and a continuous water inlet was used to gradually complete the start-up of the reactor. Main water quality parameters of the reactor inlet in Table 2. To optimize the operating conditions of the reactor, the chemical equation (2-1) was used to calculate the dosage of 1.0 times the influent nitrate concentration before the experiment. The effects of sodium thiosulfate dosage (1.0, 1.5, 2.0, 2.5), different HRTs (6, 4, 2, 1), different water pH (5, 6, 7, 8, 9), and influent temperatures on

denitrification were set. During the experimental period, the effluent concentrations of TN, NO_3^--N, NO_2^--N, and SO_4^{2-} were monitored daily. Each gradient condition was maintained for a duration of 15 days. The stoichiometric reaction is as follows:

$0.844S_2O_3^{2-} + NO_3^- + 0.347\ CO_2 + 0.\ 434\ H_2O + 0.086HCO_3^- + 0.086\ NH_4^+ \rightarrow 1.689\ SO_4^{2-} + 0.086\ C_5H_7O_2N + 0.5\ N_2 + 0.697H^+$ (2-1)

Upon reaching stable operation, packing materials were retrieved from the top, middle, and bottom sections of the reactor, designated as Samples 1, 2, and 3, respectively. Biofilm was detached from the fillers via ultrasonic vibration at 80 kHz. Following a 2-hour sedimentation period, the supernatant was decanted, and the resulting sludge precipitate was collected for 16S rRNA high-throughput sequencing.

2.3. Analytical methods

2.3.1. Conventional index analysis

The conventional indicators detected in this project test mainly included COD, TN, NH_4^+-N, NO_2^--N, NO_3^--N, and SO_4^{2-}. The analysis methods are provided in Table 3.

Table 3. Analysis method of the test.

Analysis index	Analysis method	Standard (China)
COD	Potassium dichromate method	GB 11914-1989
TN	Alkaline potassium persulfate UV spectrophotometry	HJ 636-2012
NO_3^--N	Ultraviolet spectrophotometry	HJ/T 346-2007
NO_2^--N	N- (1-naphthalene) ethylenediamine spectrophotometry	GB 7493-1987
NH_4^+-N	Sodium reagent spectrophotometry	HJ 535-2009
SO_4^{2-}	Barium chromate spectrophotometry	HJ/T 342-2007

2.3.2. X Ray fluorescence (XRF)

In this experiment, an Axios-X-ray fluorescence spectrometer of Suzhou Purui Analytical Instrument Co., LTD was used to detect the filler and analyze the proportion of the elements contained in the filler.

2.3.3. Scanning electron microscopy (SEM)

For this test, we used a German Zeiss company Auriga FIB SEM focused ion beam scanning electron microscope observation and analysis of denitrification filter packing surface morphology and growth of biofilm.

2.3.4. Microbial community analysis

To obtain the V3-V4 highly variable region of the 16S rRNA gene whose amplification primers were 338F (5'-ACTCCTACGGGAGGCAGCA-3') and 806R (5′-GGACTACHVGGGTWTCTAAT-3′) for bacterial community structure analysis, extracted genomic DNA was first amplified, and the remaining steps for high throughput sequencing and data analysis were the same as Zhou et al's study [20].

3. Results and discussion

3.1. The Influence of operating parameters on reactor denitrification

3.1.1. Effect of sodium thiosulfate dosage

The degradation effect of NO_3^--N, TN, and SO_4^{2-} with varying sodium thiosulfate dosages in the reactor are shown in Fig. 2. The optimal dosage of sodium thiosulfate was obtained by analyzing the denitrification effects of different dosages of sodium thiosulfate. During the experimental study, the concentrations of NO_3^--N, TN, and SO_4^{2-} were approximately 7.0, 7.5, and 40 mg/L. Adopting the continuous water inlet method, the HRT was 2 h. Each sodium thiosulfate dosing quantity gradient running time was 15 d, for a total operating time of 60 d.

Different effects of the additive amount of sodium thiosulfate on NO_3^-N removal are shown in Fig. 2a. With increased additive amount, the removal rate of effluent NO_3^--N also increased. When the added amount was more than 1.5 times, NO_3^-N was completely removed from the water because enough sulfur sources were ensured to participate in denitrification as electron donors [21,22].

The removal effect of TN with different additive amount of sodium thiosulfate is shown in Fig. 2b. NO_3^--N and TN removal with different dosing quantities was similar, which was due to NO_3^--N being the main tailwater TN in the sewage plant, and NO_3^--N was involved in the process of denitrification by removing naturally reduced TN content at the same time. When the dosage was ≥1.5 times, most TN in the water was removed, and the effluent TN concentration was below 0.5mg/L.

Fig. 2c shows the effluent SO_4^{2-} concentration with different sodium thiosulfate dosages. SO_4^{2-} concentration in the water with increasing additive also appeared to rise. According to the autotrophic denitrification equation involving sodium thiosulfate, the removal of 1 mg of NO_3^-N yielded 11.538 mg of SO_4^{2-} [23]. The added value of SO_4^{2-} in the water was higher than the theoretical added value, which may be due to the fact that thiobacillus and sulfur bacteria use oxygen as an electron acceptor to promote the oxidation of $S_2O_3^{2-}$ in the reactor [24], resulting in a higher concentration of SO_4^{2-} in the water.

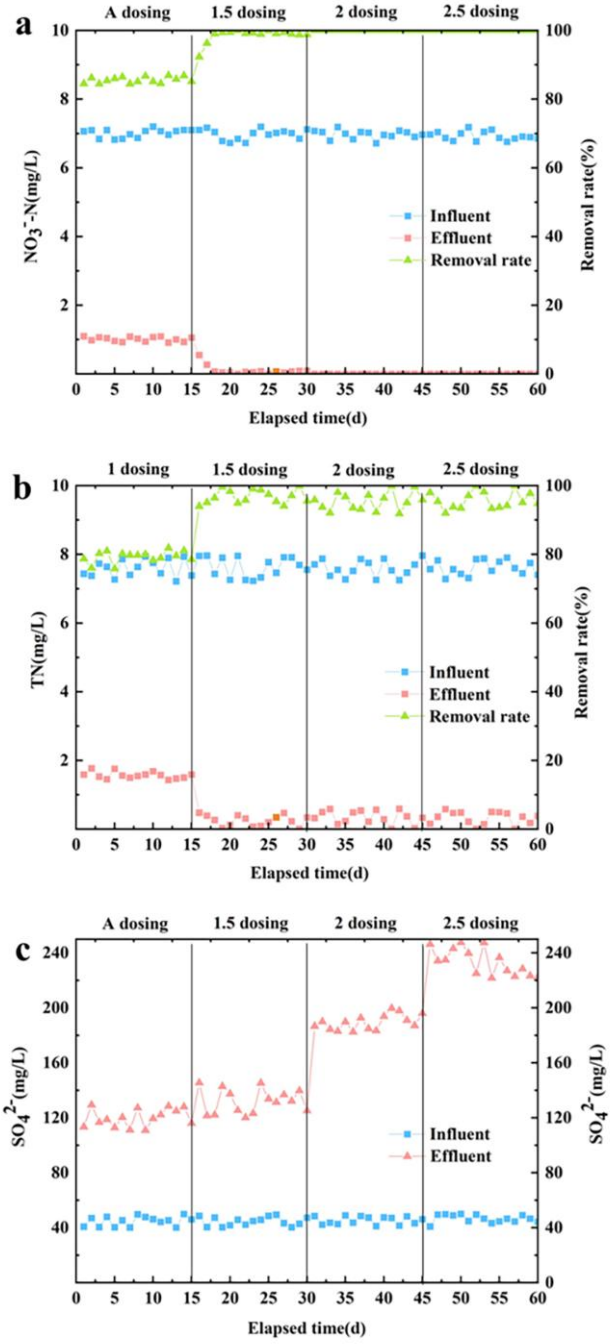


Figure 2. a: Discharge effect of NO_3^--N using different dosages of sodium thiosulfate; b: Removal effect of TN using different dosages of sodium thiosulfate; and **c:** Effluent concentration of SO_4^{2-} using different dosages of sodium thiosulfate.

In summary, increasing the sodium thiosulfate dosage to 1.5 times the theoretical stoichiometric requirement resulted in a nitrate-nitrogen (NO_3^--N) removal rate of 99.9% and a total nitrogen (TN) removal rate of 95%. Concurrently, the effluent sulfate (SO_4^{2-}) concentration remained below 250 mg/L, complying with the regulatory limit for drinking water [25]. Consequently, balancing economic feasibility with denitrification efficiency [26], the optimal sodium thiosulfate dosage for the reactor influent was determined to be 1.5 times the theoretical value.

3.1.2. Effect of HRT

In this experiment, the denitrification effect of the reactor was studied under the HRT of 6, 4, 2, and 1 h, respectively. During the experimental study, the concentration of NO_3^--N was approximately 7.0 mg/L, and the concentration of TN was about 7.5mg/L. An amount of 1.5 times the theoretical dosage of sodium thiosulfate was added to the inlet. The HRT was adjusted according to the inlet flow. The optimization phase of each HRT run was 15 d, for a total of 60 d.

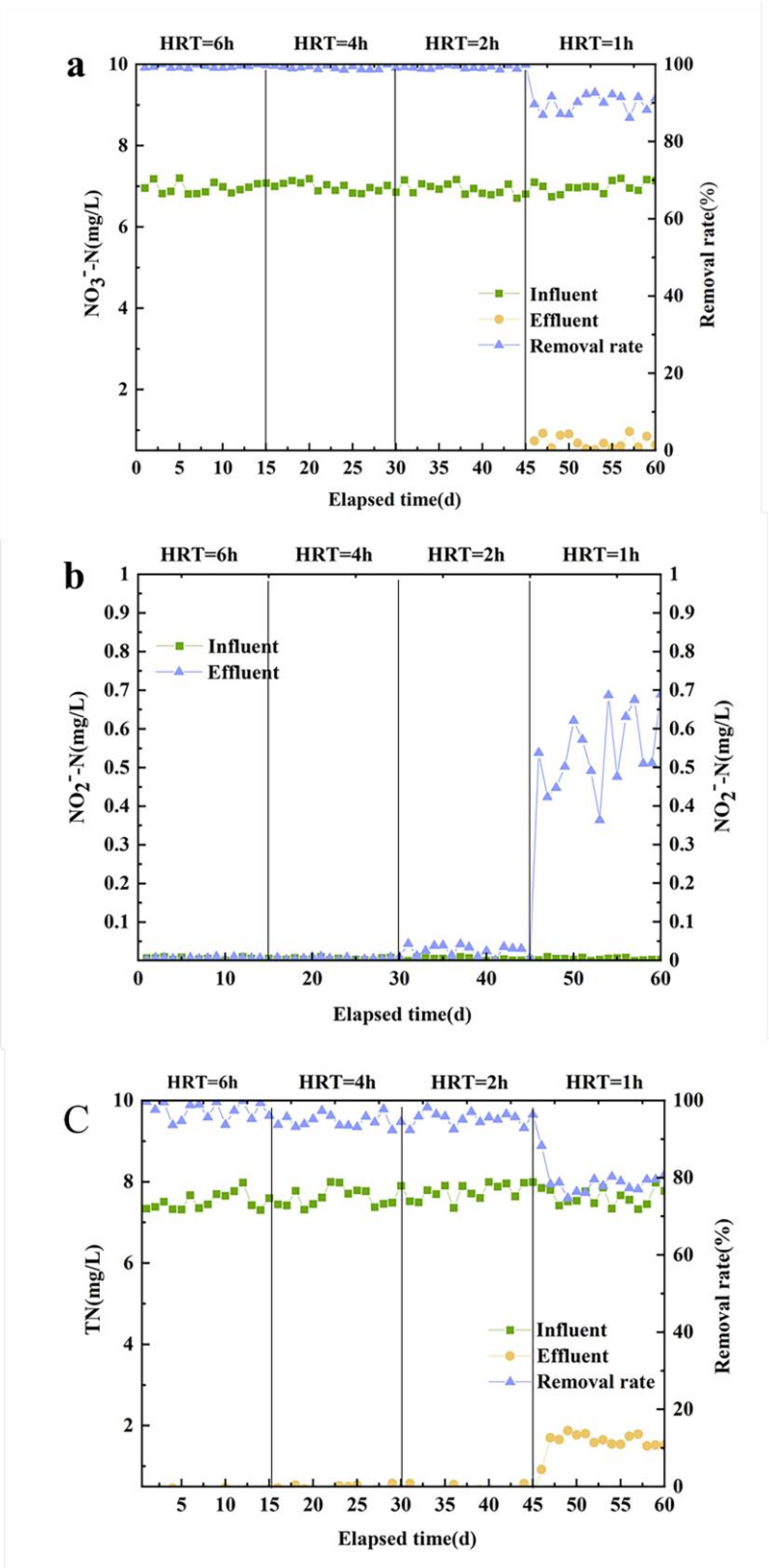


Figure 3. a: Removal effect of NO_3^--N with different conditions of HRT; b: Removal effect of TN with different conditions of HRT; and **c:** Removal effect of NO_2^--N with different conditions of HRT.

Shortening HRT affected the denitrification rate of the reactor. In Fig. 3a, when HRT was 2 to 6 h, NO_3^--N removal rate was stable at about 99.9%. When HRT was 1 h, NO_3^--N removal rate was stable at about 90.0%. This phenomenon can be attributed to the sufficiently long hydraulic retention time (HRT), which enables complete reactor filling and ensures intimate contact between aqueous NO_3^--N and the biofilm attached to the packing. Consequently, this facilitates the complete reduction of denitrification intermediates into N_2 [27].

In Fig. 3b, it is seen that the removal effect of TN was best when HRT was 2~6. On the one hand, low HRT produces a high hydraulic load, and the load on the packing of the microbial impact is larger, affecting the biomass in the reactor and resulting in a decline in the denitrification rate; on the other hand, with a short HRT, the reactor system in the denitrification process of nitrogen transformation was not sufficient, resulting in the accumulation of some other nitrogen and leading to an increased concentration of effluent TN [28].

The discharge effect of NO_2^--N under varying HRT in the reactor is shown in Fig. 3c. When HRT was 1h, the concentration of NO_2^--N in the effluent increased significantly, that is, the transformation of NO_3^--N followed the general process of biological denitrification, that is, NO_3^--N → NO_2^--N → NO → N_2O → N_2 [29]. According to Fig.3, 90% of NO_3^--N in the water was first converted to NO_2^--N, and NO_2^--N can coexist in the denitrification system and maintains a certain competitive relationship. In addition, for autotrophic denitrifying microorganisms, NO_3^--N is easier to utilize than NO_2^--N and is preferentially involved in denitrification. When the nitrate concentration in the system exceeded 70 mg/L, it can inhibit the synthesis of nitrite reductase and activity, an effect of the NO_2^--N reduction process. Combined with the above analysis, when HRT was 1 h, the water did not stay in the reactor long enough. In full consideration of the reactor operation energy consumption and the denitrification performance based on [30], the best HRT reactor time was 2 h.

3.1.3. Effect of PH

In this experiment, HRT was 2 h, and the other conditions were the same as above. During this optimization phase, the running time for each pH condition was 15 d, and the total running time was 75 d.

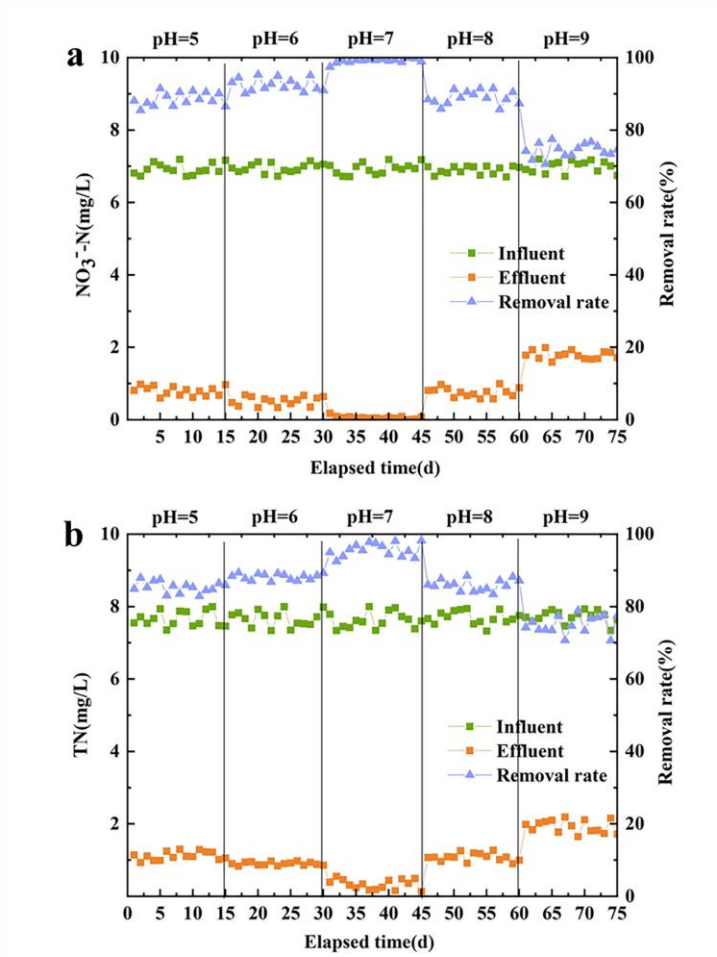


Figure 4. a: Removal effect of NO_3^--N using different conditions of pH; and **b:** Removal effect of TN using different conditions of pH.

The NO_3^--N removal effects of the reactor under varying pH conditions are shown in Fig. 4a. The reactor water pH was 7, the reactor effluent NO_3^--N concentration was the lowest, the denitrification effect was best, and the optimum pH of autotrophic denitrifying microorganisms was neutral, conforming to the denitrification of *Thiobacillus* in the living environment at this pH. When the reactor water pH was less than 7, the reactor in the system of siderite packing of acidic water could not only play a buffer role but also counteracted H^+ autotrophic denitrification, so pH was 5 and 6, and the NO_3^--N discharge rate reached more than 88%. When pH was 8, the NO_3^--N discharge rate was 88.9%, indicating that autotrophic denitrifying microorganisms in a slightly alkaline water environment to alkalinity have a certain degree of tolerance. However, when the pH value of the influent reached 9, the NO_3^--N removal rate fell to 74.4%; in the reactor, low or high pH values have a significant impact on denitrification efficiency [31].

NO_3^--N and TN removal with different pH running conditions was similar, as shown in Fig. 4b. When the water pH was maintained at 5-9, the TN removal rate was guaranteed above 70%, and denitrifying microorganisms under pH of 5-9 could maintain a certain level of activity, indicating that the removal rate of the denitrification system within this water pH range increased. To comprehensively evaluate the denitrification performance of the system, the optimal influent pH for the reactor was 7.

3.1.4. Effect of Temperature on Reactor Denitrification

In this section, we studied the denitrification effect of the reactor at different inlet temperatures. The test phase was run for a total of 90 d, and water temperature and effluent NO_3^--N and TN concentrations were monitored every 5 d. The reactor temperature varied with season. In Fig.5, as temperature reduced, the NO_3^--N, TN removal rate significantly reduced. However, relative to NO_3^--N discharge rate, fluctuation of the TN discharge rate was larger, and the effect of the temperature was more obvious.

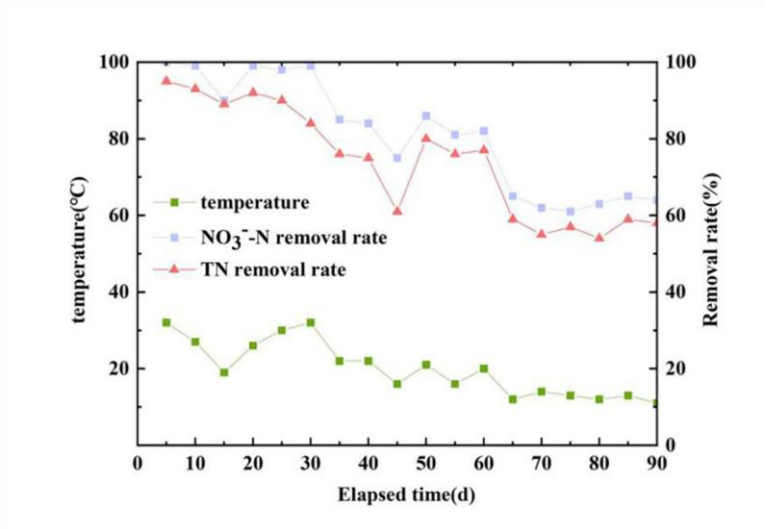


Figure 5. Discharge effect of NO_3^-N on TN using varying conditions of temperature.

When the reactor inlet temperature was near 30℃, the reactor effect was the best, and the NO_3^--N discharge rate reached 100%, in accordance with the optimal survival temperature of autotrophic denitrifying microorganisms. In terms of the effect of temperature on TN, a possible explanation is that the low temperature required for denitrifying microorganisms limits their metabolic activity and reproduction rate [32]. Relevant studies have shown that when the water temperature is lower than 20℃, the enzyme activity of microorganisms in the reactor will be inhibited, and the species of microorganisms will be reduced accordingly, which influences the denitrification process [33]. When considering the system effects on microbial activity in the denitrification reactor, the optimum temperature of the reactor inlet was 30 ℃.

3.2. Surface morphology characterization of the filler

To further analyze the surface morphology and microbial morphology of the filler in the reactor system, a SEM was used to scan and observe the filler. Through the characterization of the surface morphology of the filler in different periods, the changes in the reactor filler and microbial morphology were identified.

The SEM diagram of the original packing is shown in Fig. 6a and 6b. When the packing surface was observed at a magnification of 500 times, the packing surface structure was compact and had good integrity. When magnified 1000 times, observation of the filler surface, rough packing surface, distribution, and a large gap indicated advantages for the microbial load and growth, and these factors protected the biological membrane under higher back-flushing intensity to prevent it from easily falling off.

As shown in Fig. 6c and 6d, at 500 times magnification, many uneven folds and cavity structures existed on the packing surface. The reason may be that, on the one hand, the carbonate in the packing participated in neutralizing the process of denitrification acid production; on the other hand, the ferrous ions in the packing participated during the denitrification process, resulting in a certain quantity loss of the packing. Siderite packing not only acts as a buffer pH adjustment system as it can also be used as an electron donor to directly promote denitrification. Magnified 1000 times, packing surface supported many microorganisms, which were connected together by a viscous material and tightly attached to the packing surface.

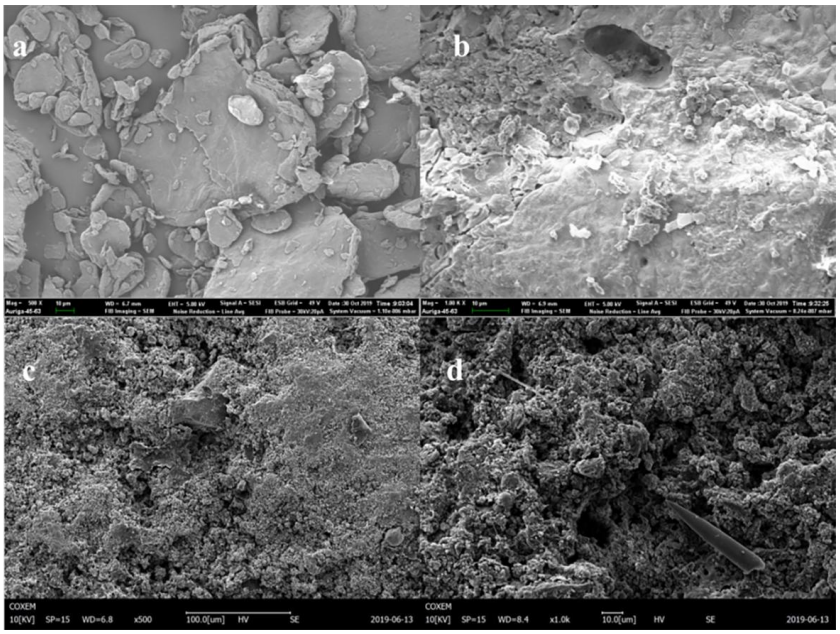


Figure 6. a, b: SEM of the original filler (a ×10000, a ×5000); and c, d: SEM of the filler in operational stage (c ×500, d ×1000).

3.3. Microbial community analysis

Microbial samples were collected from the reactor after steady-state performance was achieved under the following conditions: The reactor had been operated for 60 d with a HRT of 2 h and a temperature of 20±°C; we took 3 biological samples from the bottom to equidistant on the surface of the packing inside the reactor, and the types and abundances of the microbial communities of samples 1, 2, and 3 at different species classification levels (phylum, genus) were analyzed. In this section, we mainly present the species with the highest abundance in each sample, and the remaining species belonged to other classifications. As shown in Fig. 7a, in the community structure of samples 1, 2 and 3, *Proteobacteria* was the most abundant phylum, with an abundance of 42.78%, 46.95%, and 56.36%, respectively. This was consistent with the microbial community structure in the reactor obtained by Zhang et al. [34].

Inside the reactor, the abundance of the dominant *Proteobacteria* decreased from bottom to top, and a possible reason for this is that most autotrophic denitrifying bacteria in the reactor system are *Proteobacteria*, and as autotrophic denitrification electron acceptors decrease during the process with NO_3^--N concentrations along the reactor, there was a lower *Proteobacteria* abundance [35]. *Chloroflexi* is a facultative anaerobic bacterium that uses 3-hydroxypropionic acid to fix carbon dioxide. Moreover, some bacteria can transform nitric nitrogen into nitrous nitrogen [36].

Bacteroidetes is mainly found in anoxic environments and can participate in autotrophic denitrification reactions [37]. Therefore, the presence of such microorganisms in the reactor to some extent promotes the removal of nitrogen pollutants in the influent [38].

The genus community structure analysis is shown in Fig. 7b. In the microbial community structure of samples 1, 2, and 3, the dominant bacteria genera were *Thiobacillus* and *Ferritrophicum*, both of which belong to *Betaproteobacteria*. Moreover, *Thiobacillus* abundances were 14.83%, 16.15%, and 21.50%; *Ferritrophicum* abundances were 9.96%, 10.32%, and 9.58%, respectively. The most abundant species, *Thiobacillus,* showed abundance decreases from bottom to top. A possible reason is that *Thiobacillus* species include all kinds of obligate autotrophic microbes, and intermediate product sulfide in the reaction can be oxidized to elemental sulfur or sulfates, or undergo thiosulfate oxidation for sulfate, including in *Thiobacillus denitrificans*, which contains a complete sulfur autotrophic denitrification process and uses elemental sulfur and sulfide and thiosulfate electron donors to reduce nitrate nitrogen [39]. The path resulted in the decrease of nitrate nitrogen in water, and nitrate was an available electron acceptor for *Thiobacillus*, whose abundance also decreased. *Ferritrophicum* was highly abundant inside the reactor and showed little change along the path, possibly because siderite in the packing can provide stable ferrous ions for denitrification as electron donors. Fabisch et al. [40,41] found *Ferritrophicum* in stream sediments and identified it as neutral FeOB (iron-oxidizing bacteria) that can oxidize Fe^{2+} to Fe^{3+} with nitrate nitrogen as an electron acceptor under anaerobic conditions [42]. Such microbes can play a role in producing iron oxide under aerobic and anaerobic conditions, and the energy required to achieve growth can produce a large surface area with larger amounts of amorphous iron oxide, therefore resulting in effective adsorption of organic matter. This indicates that *Ferritrophicumlikely* played a pivotal role in the sulfur- and iron-driven denitrification processes observed in this study. Moreover, while functional gene analysis was not performed, the taxonomic composition aligned well with the observed stoichiometry.

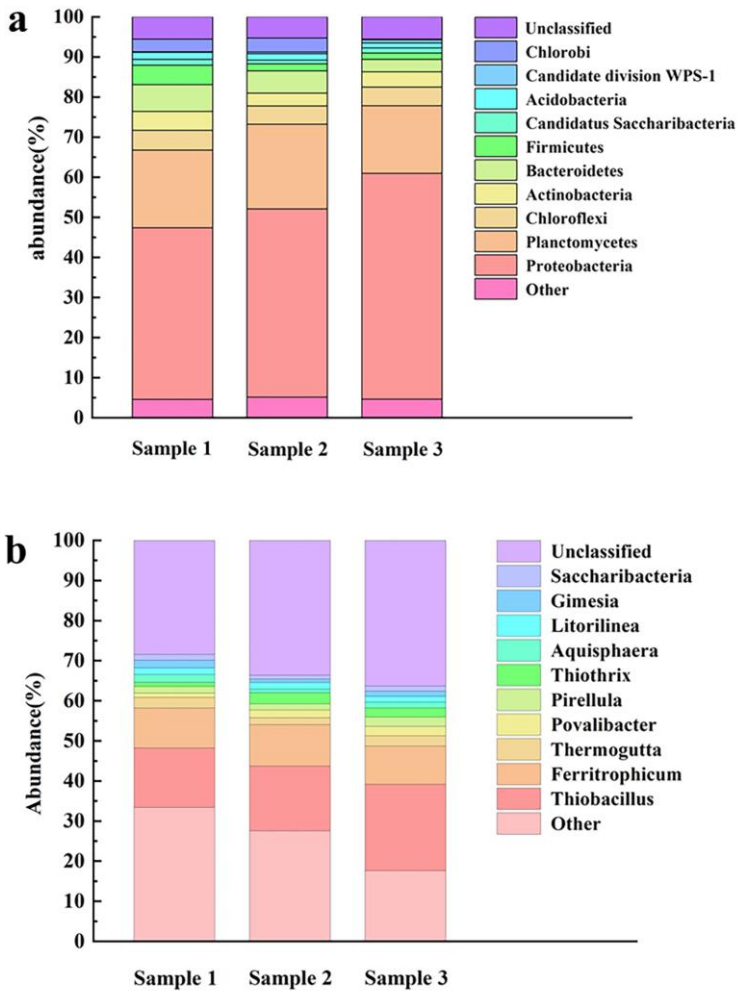


Figure 7. a: Bacterial phylum classification; and b: Taxonomic classification of the bacteria at the genus level.

3.4. Stoichiometric and biological evidence

Parallel control experiments were not conducted in this continuous-flow study. The synergistic effect of the dual electron donors is supported by stoichiometric and biological evidence.

- Stoichiometric Evidence: Theoretically, autotrophic denitrification using only $S_2O_3^{2-}$ requires a specific molar ratio of S/N, while using only Fe^{2+} requires a different Fe/N ratio. In this study, the calculated electron equivalence were derived from the consumed $S_2O_3^{2-}$ and oxidized Fe^{2+}, respectively. This indicates that both substrates actively participated in the denitrification process.
- Thermodynamic and pH Stability: The stability of the effluent pH (~7.0) without external alkalinity addition further corroborates the synergy. The acidification generated by thiosulfate oxidation ($S_2O_3^{2-} + 2O_2 + H_2O \rightarrow 2SO_4^{2-} + 2H^+$) was effectively neutralized by the protons consumed during siderite oxidation ($FeCO_3 + 0.25O_2 + 2.5H_2O \rightarrow Fe(OH)_3 + HCO_3^- + H^+$). This self-buffering capacity is a distinct characteristic of the coupled S-Fe system, distinguishing it from single-substrate systems.

Dissolved iron species were not continuously monitored in this study; the contribution of the iron pathway is supported by the electron balance analysis. Theoretically, complete denitrification driven solely by thiosulfate requires a molar ratio of 0.88. However, the actual molar ratio in this study was only 0.65. This deficit in sulfur-derived electrons implies that approximately 20% of the electrons were derived from the oxidation of Fe^{2+} released by siderite dissolution. Therefore, while direct aqueous iron measurements were absent, the stoichiometric and solid-phase evidence collectively supported the occurrence of Fe-mediated autotrophic denitrification.

4. Conclusion

To address the variability in operating conditions across studies, we evaluated the technical feasibility of the developed Sodium Thiosulfate-Siderite Autotrophic Denitrification (STSAD) biofilter using normalized performance metrics rather than removal efficiency alone. Specifically, we compared the Nitrogen Removal Rate (NRR), electron donor utilization efficiency, and byproduct accumulation (sulfate) against reported values for sulfur-, iron-, and hydrogen-based systems. Under optimized HRTs, the STSAD system achieved a competitive NRR of 7.6 g N/(m^3·d), which accounts for differences in nitrogen loading rates among reactor configurations. While maintaining high nitrogen removal performance ((NO_3^-- N) removal ~100%; TN removal >95%), the system demonstrated superior operational stability by strictly controlling effluent sulfate (≤250 mg/L) and nitrite (≤0.03 mg/L) levels, mitigating the common issue of secondary pollution in sulfur-driven processes. Furthermore, driven by the innovative "sulfur-iron synergistic metabolism," this "one-dose-dual-effect" mechanism enhances the comprehensive feasibility of the STSAD system for deep nutrient removal, offering a robust solution that balances high loading capacity with effluent safety.

Use of AI tools declaration

The authors declare they have not used Artificial Intelligence (AI) tools in the creation of this article.

Acknowledgments

Most of this work has received support from specialized scientific and technological expertise. Henan Department of Science and Technology (222102320089).

Conflict of interest

The authors declare no conflict of interest.

References

1. Li X, Zou J, Zhang D, Xie L, et al. (2021) A new method for in-situ treatment of waste gas scrubbing liquid containing both NH_3 and H_2S based on sulfur autotrophic denitrification and partial nitrification-Anammox coupling system. *Bioresource Technol* 329: 124925. https://doi.org/10.1016/j.biortech.2021.124925

2. Chen JF., Liu SN, Yan J, et al. (2017) Intensive removal efficiency and mechanisms of carbon and ammonium in municipal wastewater treatment plant tail water byozone oyster shells fix-bed bioreactor-membrane bioreactor combined system. *Ecol Eng* 101: 75–83. https://doi.org/10.1016/j.ecoleng.2016.11.029
3. Sun Y, Zhou P, Zhang N, Zhang Z, et al. (2021) Effects of matrix modification and bacteria amendment on the treatment efficiency of municipal tailwater pollutants by modified vertical flow constructed wetland. *J Environ Manage* 281: 111920. https://doi.org/10.1016/j.jenvman.2020.111920
4. Lehman SG, Badruzzaman M, Adham S, et al. (2008) Perchlorate and nitrate treatment by ion exchange integrated with biological brine treatment. *Water Res* 42: 969–976. https://doi.org/10.1016/j.watres.2007.09.011
5. Sahinkaya E, Dursun N, Kilic A, et al. (2011) Simultaneous heterotrophic and sulfur-oxidizing autotrophic denitrification process for drinking water treatment: Control of sulfate production. *Water Res* 45: 6661–6667. https://doi.org/10.1016/j.watres.2011.09.056
6. Wang Q, Gao Y, Huang H, et al. (2020) Does electrolysis facilitate simultaneous nitrogen removal and toxicity reduction of low C/N dyeing wastewater by sulfur-based denitrification biofilter? *Sci Total Environ* 722: 137898. https://doi.org/10.1016/j.scitotenv.2020.137898
7. Li Y, Wang Y, Wan D, et al. (2020) Pilot-scale application of sulfur-limestone autotrophic denitrification biofilter for municipal tailwater treatment: Performance and microbial community structure. *Bioresource Technol* 300: 122682. https://doi.org/10.1016/j.biortech.2019.122682
8. Ahmed Z, Kim SM, Kim IS, et al. (2012) Nitrification and denitrification using biofilters packed with sulfur and limestone at a pilot-scale municipal wastewater treatment plant. *Environ Technol* 33: 1271–1278. https://doi.org/10.1080/09593330.2011.619581
9. Sahinkaya E, Dursun N. (2012) Sulfur-oxidizing autotrophic and mixotrophic denitrification processes for dr＆inking water treatment: Elimination of excess sulfate production and alkalinity requirement. *Chemosphere* 89: 144–149. https://doi.org/10.1016/j.chemosphere.2012.05.029
10. Weber KA, Achenbach LA, Coates JD. (2006) Microorganisms pumping iron: anaerobic microbial iron oxidation and reduction. *Nat Rev Microbiol* 4: 752–764. https://doi.org/10.1038/nrmicro1490
11. Yang Y, Chen T, Zhang X, et al. (2018) Simultaneous removal of nitrate and phosphate from wastewater by siderite based autotrophic denitrification. *Chemosphere* 199: 130–137. https://doi.org/10.1016/j.chemosphere.2018.02.014
12. Zhu TT, Cheng HY, Yang LH, et al. (2018) Coupled Sulfur and Iron (II) Carbonate-Driven Autotrophic Denitrification for Significantly Enhanced Nitrate Removal. *Environ SciTechnol* 53: 1545–1554. https://doi.org/10.1021/acs.est.8b06865
13. Wang W, Wei D, Li F, et al. (2019) Sulfur-siderite autotrophic denitrification system for simultaneous nitrate and phosphate removal: From feasibility to pilot experiments. *Water Res* 160: 52–59. https://doi.org/10.1016/j.watres.2019.05.054
14. Di Capua F, Ahoranta SH, Papirio S, et al. (2016) Impacts of sulfur source and temperature on sulfur-driven denitrification by pure and mixed cultures of Thiobacillus. *Process Biochem* 51: 1576–1584. https://doi.org/10.1016/j.procbio.2016.06.010
15. Zhang TC, Zeng H (2006) Development of a Response Surface for Prediction of Nitrate Removal in Sulfur–Limestone Autotrophic Denitrification Fixed-Bed Reactors, *J Environ Eng-Asce* 132: 1068–1072. https://doi.org/10.1061/(ASCE)0733-9372(2006)132:9(1068)

16. Chang M, Fan F, Zhang K, et al. (2023) Denitrification performance and mechanism of a novel sulfur-based fiber carrier fixed-bed reactor: Co-existence of sulfur-based autotrophic denitrification and endogenous denitrification. *J Water Process Eng* 53: 103618. https://doi.org/10.1016/j.jwpe.2023.103618
17. XU WY (2024) Deciphering the denitrification performance and characterization of sulfur autotrophic denitrification community through metagenome: *Jiangnan University*, 2025.
18. Kelly DP, Wood AP. (2000) Confirmation of Thiobacillus denitrificans as a species of the genus Thiobacillus, in the beta-subclass of the Proteobacteria, with strain NCIMB 9548 as the type strain. *Int J Syst Evol Microbiol* 50: 547–550. https://doi.org/10.1099/00207713-50-2-547
19. Fan C, Zhou W, He S, et al. (2021) Sulfur transformation in sulfur autotrophic denitrification using thiosulfate as electron donor. *Environ Pollut* 268: 115708. https://doi.org/10.1016/j.envpol.2020.115708
20. Nisola GM, Redillas MC, Cho E, et al. (2011) Comparison of reactive porous media for sulfur-oxidizing denitrification of high nitrate strength wastewater. *Biochem Eng J* 58: 79–86. https://doi.org/10.1016/j.bej.2011.08.016
21. Khanongnuch R, Di Capua F, Lakaniemi AM, et al. (2018) Effect of N/S ratio on anoxic thiosulfate oxidation in a fluidized bed reactor: Experimental and artificial neural network model analysis. *Process Biochem* 68: 171–181. https://doi.org/10.1016/j.procbio.2018.02.018
22. Zhou W, Sun Y, Wu B, et al. (2011) Autotrophic denitrification for nitrate and nitrite removal using sulfur-limestone. *J Environ Sci* 23: 1761–1769. https://doi.org/10.1016/S1001-0742(10)60635-3
23. Qian ZM，Sun YL，Zhang XN，et al. (2023) Application of sulfur − based functional materials in advanced nitrogen removal for wastewater: Research progress and development tendency. *Energy Environ Prot* 37: 1–15.
24. HOU LN. (2022) Study on vertical flow constructed wetland with iron/manganese ore wood substrates for treatment of nitrogen-containing composite polluted wastewater: *Jilin University*, 2024.
25. Chung J, Amin K, Kim S, et al. (2014) Autotrophic denitrification of nitrate and nitrite using thiosulfate as an electron donor. *Water Res* 58: 169–178. https://doi.org/10.1016/j.watres.2014.03.071
26. Hao T, Wei L, Lu H, et al. (2013) Characterization of sulfate-reducing granular sludge in the SANI process, *Water Res* 47: 7042–7052. https://doi.org/10.1016/j.watres.2013.07.052
27. Torrentó C, Cama J, Urmeneta J, et al. (2010) Denitrification of groundwater with pyrite and Thiobacillus denitrificans. *Chem Geol* 278: 80–91. https://doi.org/10.1016/j.chemgeo.2010.09.003
28. Koenig A, Liu LH. (2002) Use of limestone for pH control in autotrophic denitrification: continuous flow experiments in pilot-scale packed bed reactors. *J Biotechnol* 99: 161–71. https://doi.org/10.1016/S0168-1656(02)00183-9
29. Xing W, He Z, Wang Y, et al. (2020) Using cold-adapted river-bottom sediment as seed sludge for sulfur-based autotrophic denitrification operated at mesophilic and psychrophilic temperatures. *Sci Total Environ* 735. https://doi.org/10.1016/j.scitotenv.2020.139345
30. Sposob M, Cydzik-Kwiatkowska A, Bakke R, et al. (2018) Temperature-induced changes in a microbial community under autotrophic denitrification with sulfide. *Process Biochem* 69: 161–168. https://doi.org/10.1016/j.procbio.2018.03.006

31. Zhang L, Zhang C, Hu C, et al. (2015) Denitrification of groundwater using a sulfur-oxidizing autotrophic denitrifying anaerobic fluidized-bed MBR: performance and bacterial community structure. *Appl Microbiol Biot* 99: 2815–2827. https://doi.org/10.1007/s00253-014-6113-9
32. Zhu Y, Wu M, Gao N, et al. (2016) Impacts of nitrate and electron donor on perchlorate reduction and microbial community composition in a biologically activated carbon reactor. *Chemosphere* 165: 134–143. https://doi.org/10.1016/j.chemosphere.2016.08.078
33. Ye L, Shao MF, Zhang T. et al. (2011) Analysis of the bacterial community in a laboratory-scale nitrification reactor and a wastewater treatment plant by 454-pyrosequencing. *Water Res* 45: 4390–4398. https://doi.org/10.1016/j.watres.2011.05.028
34. Yamada, T., Sekiguchi, Y., Hanada, S., et al. (2006) Anaerolinea thermolimosa sp. nov., Levilinea saccharolytica gen. nov., sp. nov. and Leptolinea tardivitalis gen. nov., sp. nov., novel filamentous anaerobes, and description of the new classes Anaerolineae classis nov. and Caldilineae classis nov. in the bacterial phylum Chloroflexi. *Int J Syst Evol Microbiol* 56: 1331–1340. https://doi.org/10.1099/ijs.0.64169-0
35. Wang Q, Feng C, Zhao Y, et al. (2009), Denitrification of nitrate contaminated groundwater with a fiber-based biofilm reactor. *Bioresource Technol* 100: 2223–2227. https://doi.org/10.1016/j.biortech.2008.07.057
36. Fabisch M, Beulig F, Akob DM, et al. (2013) Surprising abundance of Gallionella-related iron oxidizers in creek sediments at pH 4.4 or at high heavy metal concentrations. *Front Microbiol* 4: 390. https://doi.org/10.3389/fmicb.2013.00390
37. Zou G, Papirio S, Lakaniemi AM, et al. (2016) High-rate autotrophic denitrification in fluidized-bed biofilm reactors. *Chem Eng J* 284: 1287–1294. https://doi.org/10.1016/j.cej.2015.09.074
38. Zhang CX, Guo YK, Du HF, et al. (2016) Denitrification characteristics of a sulfur autotrophic denitrification reactor. *J Hebei Univ Sci Technol* 37: 96–101.
39. Zhang M, Zheng P, Li, et al. (2015) Performance of nitrate-dependent anaerobic ferrous oxidizing (NAFO) process: a novel prospective technology for autotrophic denitrification. *Bioresource Technol* 179: 543–548. https://doi.org/10.1016/j.biortech.2014.12.036
40. Park JH, Shin HS, Lee IS, et al. (2002) Denitrification of high NO3--N containing wastewater using elemental sulfur; nitrogen loading rate and N2O production. *Environ Technol* 23: 53–65. https://doi.org/10.1080/09593332508618431
41. Huang B, Chi G, Chen X, et al. (2011) Removal of highly elevated nitrate from drinking water by pH-heterogenized heterotrophic denitrification facilitated with ferrous sulfide-based autotrophic denitrification. *Bioresource Technol* 102: 10154–10157. https://doi.org/10.1016/j.biortech.2011.08.048
42. Zheng YC, Wang ZZ, Cao T, et al. (2022) Enhancement effects and pathways of nitrogen removal by plant-based carbon source in integrated vertical flow constructed wetlands. *J Water Process Eng* 47: 102–104. https://doi.org/10.1016/j.jwpe.2022.102734



AIMS Press

© 2026 the Author(s), licensee AIMS Press. This is an open access article distributed under the terms of the Creative Commons Attribution License (http://creativecommons.org/licenses/by/4.0)